ISSN 1027-5495. Functional Materials, 26, No.1 (2019), p. 71-77.
doi:https://doi.org/10.15407/fm26.01.71

Phase composition, structure, corrosion and radiation resistance of synthesized $Ca_{10}(PO_4)_6F_2$ and $Ca_9Sr(PO_4)_6F_2$ fluorapatites

V.A.Shkuropatenko, S.Y.Sayenko, K.A.Ulybkina, A.V.Zykova, L.M.Lytvynenko, A.G.Myronova

National Science Center "Kharkiv Institute of Physics and Technology", 1 Academichna Str., 61108 Kharkiv, Ukraine

Received July 5, 2018

The effect of electron irradiation (*E* up to 10 MeV) on the phase composition, structure, and corrosion resistance of synthesized fluorapatite was investigated in the study. Powders of calcium $Ca_{10}(PO_4)_6F_2$ and strontium-containing $Ca_9Sr(PO_4)_6F_2$ fluorapatites were synthesized by the method of co-precipitation from the solutions of the initial components. The samples of fluorapatite with a maximum value of the relative density (90–92 %) were produced by sintering in air at a temperature of 1250°C for 6 h. The secondary phase of tricalcium phosphate α–$Ca_3(PO_4)_2$ in the resulting samples was observed. Increasing the heat treatment time up to 9 h leads to a disorder in the structure of the fluorapatite. XRD analysis of glass-ceramic fluorapatite samples after electron irradiation process has shown the lines of fluorapatite and "halo" in the diffractogram, which indicates amorphization of fluorapatite samples. It has been established that electron irradiation to absorbed dose of 10^8 Gy does not significantly affect the corrosion resistance of the obtained fluorapatite samples.

Keywords: fluorapatite, matrix, electron irradiation, phase composition, structure, corrosion resistance.

Исследовано влияние электронного облучения (*E* до 10 МэВ) на фазовый состав, структуру и коррозионную стойкость синтезированного фторапатита. Порошки кальциевого $Ca_{10}(PO_4)_6F_2$ и стронцийсодержащего фторапатита $Ca_9Sr(PO_4)_6F_2$ синтезировали методом совместного осаждения из растворов исходных компонентов. Образцы фторапатита с максимальным значением относительной плотности (90–92 %) получали спеканием на воздухе при температуре 1250°C в течение 6 час. В полученных образцах наблюдалась вторичная фаза трикальцийфосфата α–$Ca_3(PO_4)_2$. Увеличение времени термообработки до 9 час приводит к нарушению структуры фторапатита. Рентгенофазовый анализ стекло-керамических образцов фторапатита после электронного облучения показал наличие линий фторапатита и "гало" на дифрактограмме, что указывает на аморфизацию образцов фторапатита. Установлено, что облучение электронами до поглощенной дозы 10^8 Гр не оказывает существенного влияния на коррозионную стойкость полученных образцов фторапатита.

Фазовий склад, структура, корозійна та радіаційна стійкість синтезованих $Ca_{10}(PO_4)_6F_2$ та $Ca_9Sr(PO_4)_6F_2$ фторапатитів. *В.А.Шкуропатенко, С.Ю.Саєнко, К.А.Улибкіна, А.В.Зикова, Л.М.Литвиненко, А.Г.Миронова*

Вивчено вплив електронного випромінювання (*E* до 10 МеВ) на фазовий склад, структуру та корозійну стійкість синтезованого фторапатиту. Порошки кальцієвого $Ca_{10}(PO_4)_6F_2$ та стронційвміщуючого фторапатиту $Ca_9Sr(PO_4)_6F_2$ синтезовано методом спільного осадження з розчинів вихідних компонентів. Зразки фторапатиту з максимальним значенням відносної густини (90–92 %) отримано спіканням на повітрі за

температури 1250°С протягом 6 год. В отриманих зразках спостерігається вторинна фаза трикальційфосфату α–$Ca_3(PO_4)_2$. Збільшення часу термообробки до 9 год приводить до порушення структури фторапатиту. Рентгенофазовий аналіз скло-керамічних зразків фторапатиту після електронного опромінення показав наявність ліній фторапатиту та "гало" на дифрактограмі, що вказує на аморфізацію зразків фторапатиту. Встановлено, що опромінення електронами до поглиненої дози 10^8 Гр не має суттєвого впливу на корозійну стійкість отриманих зразків фторапатиту.

1. Introduction

Minerals and synthetic compounds with a structural type of apatite are widely used in many fields, including biology, medicine, electronics, etc. [1–5]. Such materials also serve as catalysts and ion exchangers in the chemical industry. Apatite materials, activated by rare earth elements, are used as luminescent and laser materials. Some apatite materials have found wide application in orthopedics and dentistry, due to the composition closed to an inorganic component of human bones and teeth. Moreover, apatite materials are considered as promising materials for the immobilization of high-level waste (HLW), due to the high chemical and radiation resistance and a wide range of structural iso- and heterovalent substitutions [6].

At present, it is known that the reliable immobilization of long-lived actinides and fission products requires the formation of crystalline matrices similar to the natural analogs containing radioactive elements in the structure during geological epochs with preserving chemical and structural stability. One of the famous examples demonstrating the chemical and radiation resistance of apatite in nature is the uranium deposit in Oklo (Gabon, Africa). Composition of local rocks includes apatite. The chain reaction of uranium fission took place approximately two billion years ago. Apatite crystals from this deposit are characterized by anomalous enrichment of ^{235}U and fission products [7].

The behavior of the material under irradiation is one of the main factors, which should be considered choosing a matrix material for immobilization of HLW. The matrix included HLW will be subjected to the action of α-, β-particles and γ-radiation due to the decay of radionuclide contained waste. The structural and chemical changes at the atomic level in the solidified forms of waste under the radiation process can lead to a change in the volume, microstructure, mechanical properties of the materials, and matrix resistance to leaching [8].

It is well known, that high-energy beams of ions and electrons are widely used to simulate microstructural changes and phase transformation in ceramic materials caused by α-, β-decays, neutrons and fission products. The advantage of charged particles accelerators using is the possibility of high irradiation doses obtaining during a short time. Irradiation by a strong ion beam can be used to simulate radiation damage due to α-decay in the case of inclusion of actinides in matrix material. Damage caused by electron irradiation can be used to simulate the effects of ionization and electronic excitations from β-particles [9].

The aim of the study was research of the effect of electron irradiation on the phase composition, structure and corrosion resistance of fluorapatite materials produced by precipitation from solutions.

2. Experimental

To produce calcium fluorapatite $Ca_{10}(PO_4)_6F_2$ by precipitation method the following components were used: calcium nitrate $Ca(NO_3)_2 \cdot 4H_2O$, dibasic ammonium phosphate $(NH_4)_2HPO_4$, ammonium fluoride NH_4F, which were taken in stoichiometric proportions. In the case of synthesis of fluorapatite with strontium $Ca_9Sr(PO_4)_6F_2$, strontium nitrate $Sr(NO_3)_2$ was used as an aqueous solution. Heat treatment of powders and sintering of fluorapatite samples were carried out in air in a high-temperature electric furnace Nabertherm P310 (Germany). Phase studies were carried out using the X-ray phase analysis (XRD) method (DRON-1.5, in copper radiation using a nickel selective filter). The apparent density of the samples after sintering was determined hydrostatically in accordance with GOST 2409-195. The microstructure of the samples of fluorapatite was studied on a scanning electron microscope JSM-7001F (JEOL, Japan) equipped with a thermo-field electron gun. Electron irradiation (electron energy up to 10 MeV) was carried out at the accelerator KUT-1 (NSC KIPT). The samples of fluorapatite were irradiated by electrons to absorbed dose of 10^8 Gy.

The preparation of calcium $Ca_{10}(PO_4)_6F_2$ and strontium-containing $Ca_9Sr(PO_4)_6F_2$ fluorapatite by the precipitation method was carried out according to the following reactions, respectively:

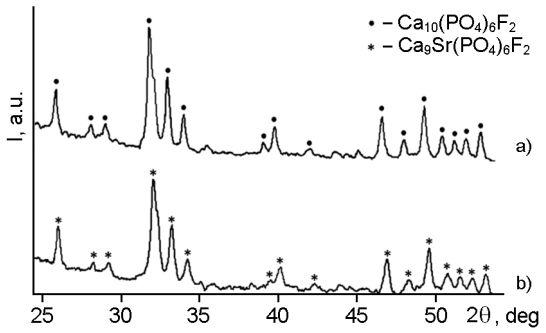

Fig. 1. XRD patterns of the initial powders: a — $Ca_{10}(PO_4)_6F_2$, b — $Ca_9Sr(PO_4)_6F_2$.

$$10Ca(NO_3)_2 + 6(NH_4)_2HPO_4 + 2NH_4F + NH_4OH + \frac{1}{2}O_2 \rightarrow Ca_{10}(PO_4)_6F_2 + 14NH_4NO_3 + 5.5H_2O + 7NO_2\uparrow \quad (1)$$

$$9Ca(NO_3)_2 + Sr(NO_3)_2 + 6(NH_4)_2HPO_4 + 2NH_4F + NH_4OH + \frac{1}{2}O_2 \rightarrow Ca_9Sr(PO_4)_6F_2 + 14NH_4NO_3 + 5.5H_2O + 7NO_2\uparrow. \quad (2)$$

The process of calcium and strontium-containing fluorapatite producing by the method of chemical co-precipitation included the following stages:

— preparation of aqueous solutions of the initial components $Ca(NO_3)_2 \cdot 4H_2O$, $(NH_4)_2HPO_4$, NH_4F and $Sr(NO_3)_2$ (for $Ca_9Sr(PO_4)_6F_2$) the required concentration;

— mixing of initial solutions. pH = 9–9.5 was adjusted by the addition of ammonium hydroxide NH_4OH;

— preparation of $Ca_{10}(PO_4)_6F_2$ and $Ca_9Sr(PO_4)_6F_2$: powders, sedimentation, decantation, washing, drying in air, grinding [10].

As previously referred [11] in Fig. 1 presents the XRD data of calcium $Ca_{10}(PO_4)_6F_2$ and strontium-containing $Ca_9Sr(PO_4)_6F_2$ fluorapatite powders produced by co-precipitation from solutions of the initial components. Analysis of the diffractograms of the produced powders indicates that the composition of the powders corresponds to the phase of $Ca_{10}(PO_4)_6F_2$ (JCPDS 15-0876) (Fig. 1a) and $Ca_9Sr(PO_4)_6F_2$ (Fig. 1b), correspondently. No secondary phases were detected.

Samples for sintering in air were prepared in the form of tablets with a diameter of 14 mm and a height of 5–7 mm by the method of cold two-sided axial pressing of synthesized fluorapatite powders on a hydraulic press. Pressing was carried out in the pressure range of 124–247 MPa. Sintering of the samples was carried out in the temperature range 1000–1250°C, for 1, 6 and 9 h in air. Fig.2 shows the relative density of the $Ca_{10}(PO_4)_6F_2$ and $Ca_9Sr(PO_4)_6F_2$ fluorapatites as a function of the sintering temperature for a fixed sintering time of 6 h. According to the results of density measurement, it was found that at a temperature of 1250°C the maximum relative density for calcium fluorapatite and fluorapatite containing strontium (90–92 %) is observed.

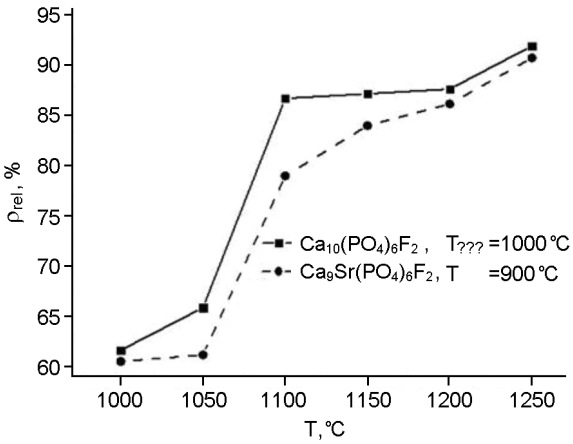

Fig. 2. The dependence of relative density of $Ca_{10}(PO_4)_6F_2$ and $Ca_9Sr(PO_4)_6F_2$ samples on the sintering temperature, time of sintering — 6 h.

Electron irradiation of calcium fluorapatite samples was performed on a linear electron accelerator KUT-1 up to a set of absorbed dose of 10^8 Gy. According to [12], a dose of $6 \cdot 10^8$ Gy can be obtained by waste glasses that will be generated at the Savannah River Plant in South Carolina at the expense of β/γ-radiation of the included radionuclides during storage up to 10^3 years. The generated high-energy electron flux with energy up to 10 MeV on the linear accelerator of electrons KUT-1 allows to collect the required dose in a short time (for example, a dose of 10^8 Gy for 12 h).

The samples of calcium fluorapatite after sintering at a temperature of 1150°C for 6 h and at a temperature of 1250°C for 9 h were selected as samples under electron irradiation. To ensure heat removal during irradiation process, the target with fluorapatite samples was cooled by water.

The appearance of $Ca_{10}(PO_4)_6F_2$ (T = 1150°C, τ = 6 h) samples irradiated with electrons did not differ from the

Fig. 3. The view of $Ca_{10}(PO_4)_6F_2$ (T = 1250°C, τ = 9 h) samples before (a) and after (b) electron irradiation process.

$Ca_{10}(PO_4)_6F_2$ (T = 1150°C, τ = 6 h) samples prior to irradiation. Irradiated samples of $Ca_{10}(PO_4)_6F_2$ (T = 1250°C, τ = 9 h) also did not differ in appearance from the samples prior to irradiation, except for color. The samples of fluorapatite sintered in air at 1250°C for 9 h were colored to blue as a result of electron irradiation to the absorbing dose of 10^8 Gy (Fig. 3).

Leaching of fluorapatite samples was carried out in a Teflon container at a constant temperature of 90°C in distilled water. The volume of distilled water in the container was determined from the ratio of surface/volume = 1/10. The distilled water changing, measurement of the weight and total surface of the samples were carried out after 3, 7, 14, 21 and 28 days. The total leaching rate V (g/m^{2}d) was calculated by the formula:

$$V = \Delta w / S \cdot t, \qquad (3)$$

where t (day) is the leaching time, Δw (gram) is the difference in sample weight before and after leaching in t days, S (m^2) is the total surface of the sample.

3. Results and discussion

Fig. 4 shows the XRD analysis of calcium and strontium-containing fluorapatite samples produced by sintering in air at 1150°C for 1 h [11]. Apparently, the sintering of calcium fluorapatite under such conditions leads to the appearance of one line of the secondary phase — tricalcium phosphate α–$Ca_3(PO_4)_2$ (JCPDS 29-0359) of low intensity (Fig. 4a). On the diffractogram of strontium-containing fluorapatite, an increase in the number of α–$Ca_3(PO_4)_2$ lines is observed (Fig. 4b).

The electron irradiation of $Ca_{10}(PO_4)_6F_2$ samples (T = 1150°C, τ = 6 h) to a dose of 10^8 Gy does not lead to a change in the

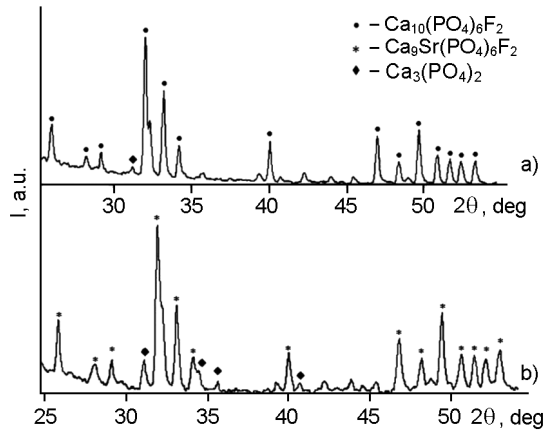

Fig. 4. XRD patterns of fluorapatite samples after sintering at the temperature 1150°C during one hour: a — $Ca_{10}(PO_4)_6F_2$, b — $Ca_9Sr(PO_4)_6F_2$.

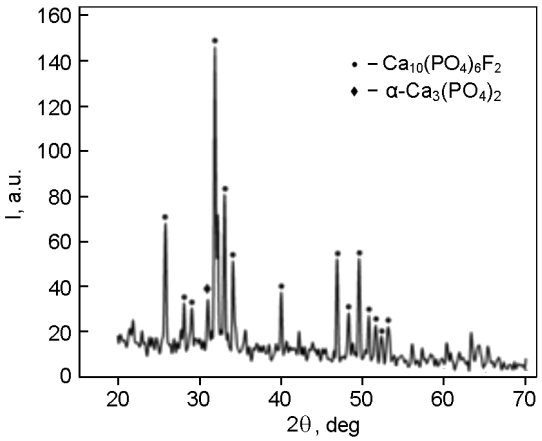

Fig. 5. XRD patterns of fluorapatite sample $Ca_{10}(PO_4)_6F_2$ after sintering at the temperature 1150°C during 6 h and electron irradiation.

phase composition of synthesized calcium fluorapatite. In addition, there is, besides the main lines of fluorapatite, the tricalcium phosphate line on the diffractogram of irradiated samples of fluorapatite (Fig. 5). The intensification of the lines of fluorapatite and the decrease in the width indicate an increase in the crystallinity of the resulting fluorapatite after sintering at a temperature of 1150°C for 6 h and irradiation with electrons.

The SEM images of the microstructure of ceramic fluorapatite samples of ($Ca_{10}(PO_4)_6F_2$) composition obtained by sintering in air at processing temperature of 1150°C and holding time of 6 h before and after electron irradiation demonstrate the presence of a uniform porous structure with

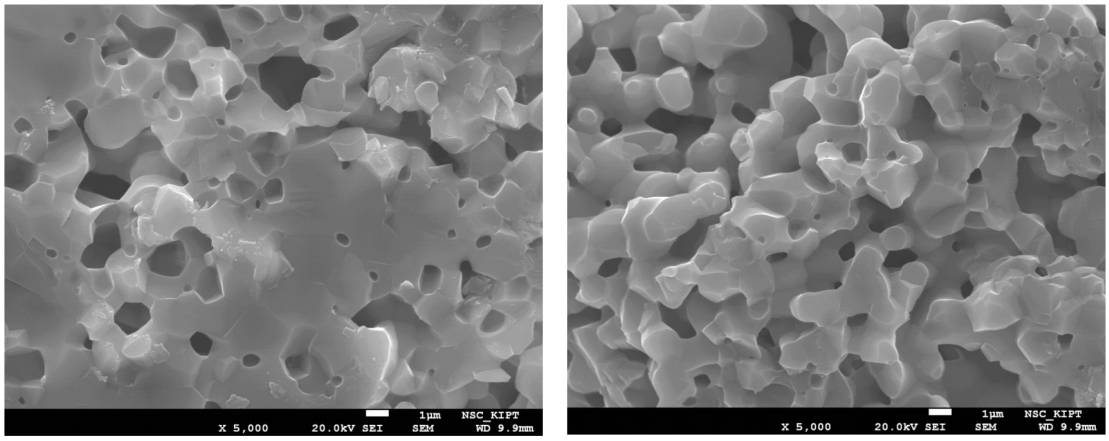

Fig. 6. SEM image of the $Ca_{10}(PO_4)_6F_2$ sample, T = 1150°C, τ = 6 h: a — before electron irradiation, b — after electron irradiation.

grains size 1–2 μm (Fig. 6a and 6b). The visible changes in the microstructure of the fluorapatite ceramic samples after electron irradiation were not observed. An increase in the sintering temperature up to 1250°C (holding time 1 h) leads to the disappearance of the tricalcium phosphate line on the diffractogram of calcium fluorapatite (Fig. 7a) and to a decrease in the intensity and number of its lines in the diffractogram of strontium-containing fluorapatite (Fig. 7b). Further crystallization of the synthesized fluorapatites occurs with a simultaneous increase in the density of the obtained samples (Fig. 2).

The increase in the sintering time up to 9 h at temperature of 1250°C results in the formation of a glass phase in calcium fluorapatite samples. The relative density of such samples decreases to 84.2 %. As can be seen in Fig. 8a, the obtained glass-ceramic material is a glass matrix with numerous pores and crystalline microinclusions of predominantly oval shape. Fig. 8b shows SEM images of the microstructure of a glass-ceramic fluorapatite sample after electron irradiation. Small pores of 10–15 μm, larger ~ 50 μm and microinclusions of 10–20 μm are visible on the microstructure images of fluorapatite samples after electron irradiation, as well as in the microphotograph of the microstructure of the unirradiated fluorapatite sample.

The presence of the glass matrix in the fluorapatite samples after sintering at a temperature of 1250°C and holding time of 9 h, resulting in the color of the samples after electron irradiation process. Glasses are characterized by the coloration under

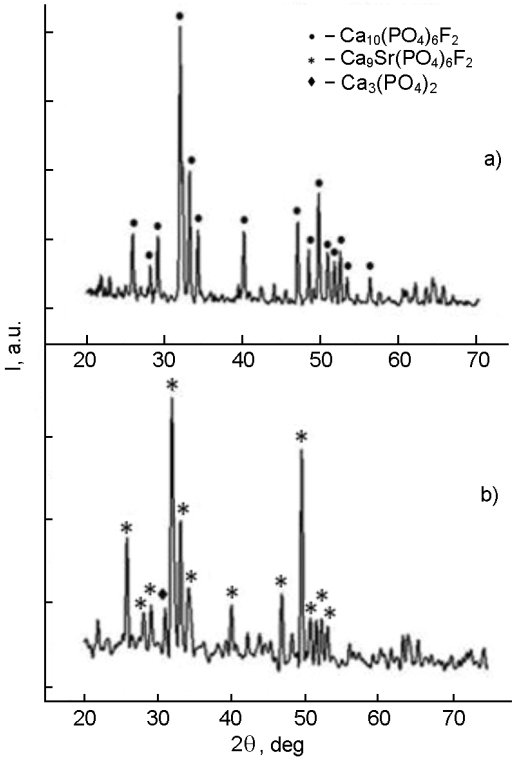

Fig. 7. XRD patterns of fluorapatite samples after sintering at the temperature 1250°C during one hour: a — $Ca_{10}(PO_4)_6F_2$, b — $Ca_9Sr(PO_4)_6F_2$.

the influence of various types of radiation, including the action of electron beams [12].

The relative density of the irradiated sample of glass-ceramic fluorapatite (83.9 %) decreases insignificantly as compared to the unirradiated sample (84.2 %). A slight decrease in the relative density of the fluorapatite samples after irradiation is also characteristic of ceramic fluorapatite samples obtained by sintering at tempera-

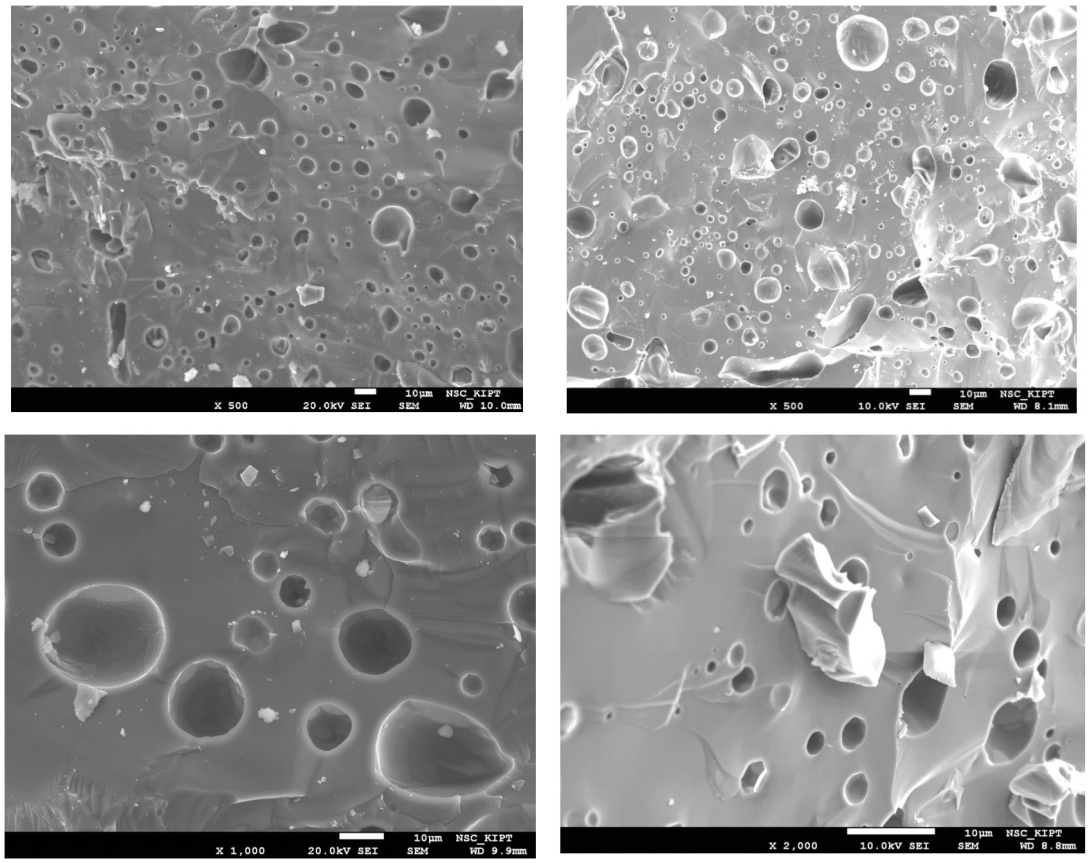

Fig. 8. SEM image of $Ca_{10}(PO_4)_6F_2$ sample (T = 1250°C, τ = 9 h): a — before electron irradiation, b — after electron irradiation.

ture of 1150°C and holding time of 6 h. Irradiation of ceramic fluorapatite samples leads to the decrease in the relative density from 86.6 % to 86.2 %. Previously, it was shown that the density and micro-hardness parameters of sodium-aluminum-phosphate glasses samples are not principally changed at doses of β- and γ-irradiation up to 10^{10} rad (10^8 Gy) [14]. Higher-doses of the electron and ions irradiation by accelerators lead to charge accumulation, and the formation of gas bubbles, similar to the process in silicate and borosilicate glasses [15–17].

XRD analysis of glass-ceramic fluorapatite samples after electron irradiation process has shown the lines of fluorapatite, one tricalcium phosphate line and "halo" in the diffractogram, which indicates amorphization of fluorapatite samples (Fig. 9).

Table shows the results of the leaching of fluorapatite samples $Ca_{10}(PO_4)_6F_2$ and $Ca_9Sr(PO_4)_6F_2$ obtained by sintering at T = 1150°C for 6 h before and after electron irradiation. As can be seen from the Table, the loss of weight and the overall leaching rate of investigated fluoropatite samples without strontium is much less than for samples with strontium. This fact is apparently due to the presence in the $Ca_9Sr(PO_4)_6F_2$ samples of more tricalcium

Table. Sizes, weight, loss, and leaching rate of the fluoropatite samples

	Diameter d, mm	Height h, mm	Initial weight w_0, g	Surface S_0, mm^2	Δw_1, g (3 days)/V, g/m^{2}d	Δw_2, g (7 days)/V, g/m^{2}d	ΔwБЬЕ 9wВ з, g (14 days)/V, g/m^{2}d	Δw_4, g (21 day)/V, g/m^{2}d	Δw_5, g (28 day)/V, g/m^{2}d
$Ca_{10}(PO_4)_6F_2$	13.5	6.5	2.0123	561.66	0.0006/0.357	0.00111/0.284	0.00141/0.183	0.00151/0.131	0.00159/0.104
$Ca_9Sr(PO_4)_6F_2$	14.5	6.5	1.5695	626.03	0.0013/0.72	0.0022/0.536	0.0026/0.342	0.00275/0.264	0.0028/0.16

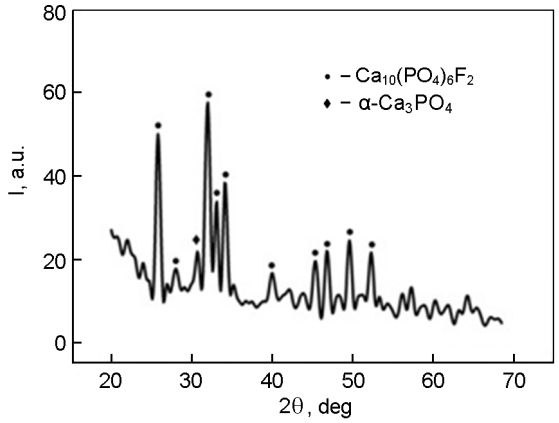

Fig. 9. XRD patterns of $Ca_{10}(PO_4)_6F_2$ sample (T = 1250°C, τ = 9 h) after electron irradiation.

phosphate α–$Ca_3(PO_4)_2$ phase, which has greater solubility in comparison with fluorapatite [18]. The leaching of the fluorapatite sample after electron irradiation showed a relatively small decrease in weight loss and leaching rate compared to the unirradiated sample. Probably, irradiation with electrons leads to additional crystallization of fluorapatite, which in turn provides a slight increase in its corrosive properties.

The obtained data showed that simulation of the electron irradiation to a dose of 10^8 Gy does not lead to a significant change in the density, corrosion resistance, structure and phase composition of the synthesized fluorapatite samples.

4. Conclusions

Powders of fluorapatite compositions ($Ca_{10}(PO_4)_6F_2$) and ($Ca_9Sr(PO_4)_6F_2$) have been synthesized by chemical precipitation. It has been established that the formation of mono phase fluorapatites $Ca_{10}(PO_4)_6F_2$ and $Ca_9Sr(PO_4)_6F_2$ during chemical precipitation occurs directly as a result of the reaction between the solutions of the initial components.

Samples of calcium and strontium-containing fluorapatite with relative density (91–92 %) were obtained by sintering in air at a temperature of 1250°C and a holding time of 6 h. The increase in the heat treatment time up to 9 h results in the change of the $Ca_{10}(PO_4)_6F_2$ sample material from crystalline to crystalline-glass phase.

Electron irradiation of the $Ca_{10}(PO_4)_6F_2$ ceramic fluorapatite samples up to the absorbed dose 10^8 Gy (E up to 10 MeV) is not principally changed the density, structure, and phase composition of ceramic and glass-ceramic fluorapatites.

Based on the results of leaching tests in the water of the fluorapatite samples, it was established that calcium fluorapatite samples showed a small decrease in weight loss and leaching rate compared to the unirradiated samples, probably due to additional crystallization of fluorapatite after electron irradiation, which in turn provides a slight increase in the corrosive properties of the samples.

The possibility of the electron irradiation (E up to 10 MeV) process using for simulation of the HLW effect on the matrix material was shown. The stability of the physicochemical properties during electron irradiation allows to consider the materials based on fluorapatite as a promising matrix for the immobilization of HLW.

References

1. A.P.Shpak, V.L.Karbovskiy, V.V.Trachevskiy, Apatites, Akademperiodika, Kiev (2002).
2. N.V.Babayevskaya, Yu.N.Savin, A.V.Tolmachev, *J. Inorg. Mater.*, **43**, 976 (2007).
3. S.Ramesha, K.L.Aw, R.Tolouei et al., *Ceram. Intern.*, **39**, 111 (2013).
4. E.Landi, A.Tampieri, G.Celotti et al., *Acta Biomater.*, **3**, 961 (2007).
5. F.Scalera, F.Gervaso, B.Palazzo et al., *Engin. Mater.*, **758**, 132 (2017).
6. O.Terra, F.Audubert, N.Dacheux et al., *J.Nucl. Mater.*, **354**, 49 (2006).
7. R.Bros, J.Carpena, V.Sereand et al., *Radiochim. Acta*, **74**, 277 (1996).
8. A.O.Merkushin, The Thetis for the Degree of Candidate of Chemical Science, Moscow (2003).
9. J.Lian, L.M.Wang, K.Sun et al., *Microscopy Res. Techn.*, **72**, 165 (2009).
10. S.Yu.Sayenko, V.A.Shkuropatenko, R.V.Tarasov et al., *Visnik NTU "KHPI"*, **28**, 117 (2014).
11. S.Yu.Sayenko, *Functional Materials*, **22** (2), 263 (2015).
12. R.C.Ewing, W.J.Weber, F.W.Clinard, *Progress Nuclear Energy*, **29(2)**, 63 (1995).
13. S.M.Brekhovskikh, Yu.N.Viktorova, L.M.Landa, Radiation Effects in Glasses, Energoizdat, Moscow (1982) [in Russian].
14. A.A.Vashman, A.S.Polyakov, Phosphate Glasses with Radioactive Waste, TsNIIAtominform, Moscow (1997) [in Russian].
15. V.A.Starodubtsev, L.N.Shiyan, A.S.Portnyagin, N.N.Zausayeva, *Phys. Chem. Glass*, **17(5)**, 816 (1991).
16. W.J.Weber, R.C.Ewing, C.F.Angell et al., *J. Mater. Res.*, **12**, 1946 (1997).
17. W.J.Weber, *Proc. Mater. Sci.*, **7**, 237 (2014).
18. T.Kanazava, Inorganic Phosphate Materials, Naukova Dumka, Kiev (1998).